The Pennsylvania State University

The Graduate School

STUDY OF TRANSFER ENTROPY ON EPILEPTIC EEG SIGNALS

A Thesis in

Electrical Engineering

by

Poojitha Kale

Submitted in Partial Fulfillment
of the Requirements
for the Degree of

Master of Science

May 2019

The thesis of Poojitha Kale was reviewed and approved* by the following:

Aylin Yener
Distinguished Professor of Electrical Engineering and Dean's Fellow
Thesis Co-advisor

Mohamed Almekkawy
Assistant Professor of Computer Science and Engineering
Thesis Co-advisor

Thyagarajan Subramanian
Professor of Neurology and Neural and Behavioral Sciences at Penn State College of Medicine
Director, Central PA APDA Informational Center and Movement Disorders Program at Penn State College of Medicine

Kultegin Aydin
Professor of Electrical Engineering
Head of the Department of Electrical Engineering

*Signatures are on file in the Graduate School

ABSTRACT

Epilepsy is the fourth largest neurological disorder characterized by recurrent unprovoked seizures. The usual brain activity is disturbed for the duration of the seizure which can last a few seconds up to a few minutes. About one-third of the people suffer from medically refractory seizures. This means that medication alone cannot make the patient seizure free. These patients are often evaluated for surgery where the focus of the epileptogenic zones (EZs) are resected. Identification of these EZs is made easy by subjecting the patients to an invasive EEG monitoring method, where multiple intra-cerebral depth electrodes are used to capture the electrical activity of the brain. In this thesis, an alternate method named Transfer Entropy (TE) is proposed over the standard method of evaluating these signals by visually identifying the changes in the EEG signal. This method accurately accounts for non-linearity and dynamic interactions between the systems involved. By applying this method to the EEG data of four epileptic patients, the location of EZs for each patient was identified. In addition to this, investigation on the changes in the TE calculations by changing parameters such as the bin size and the order of the Markov processes has been studied. Computation and comparison of both the linear (Correlation) and non-linear (TE) calculations have been shown to show why this particular method proves to be more useful.

TABLE OF CONTENTS

LIST OF FIGURES

LIST OF TABLES

ACKNOWLEDGEMENTS

First and foremost, I would like to thank my advisors, Professor Aylin Yener and Professor Mohamed Almekkawy for their guidance and support throughout my Master's program. I would also like to thank Dr Thyagarajan Subramanian and Dr Jayant Acharya for providing me with the relevant medical knowledge and data for this research. Special thanks to all the group members of the Ultrasound in Imaging and Therapy (UIT) lab – James, Navid, Shaikhah, Bharadwaj, Xingzhao, Xiaoyu and Hanan. This work would not have been possible without the strong collaboration between the EECS department at University Park and the Penn State School of Medicine at Hershey. Thank you for inspiring and motivating my work.

Lastly, I would like to thank my parents and my brother, without whose support this entire journey would not have been possible. I would also like to thank my friends and roommates for motivating me. Thank you for believing in me.

Chapter 1

Introduction

1.1 Epilepsy:

Epilepsy is the fourth most common neurological disorder after migraine, stroke and Alzheimer's disease. World health organization defines Epilepsy as 'a disorder of the brain characterized by an enduring predisposition to generate epileptic seizures, and by the neurobiological, cognitive, psychological and social consequences of this condition. The definition of epilepsy requires the occurrence of at least one epileptic seizure'[1][2]. The seizures are caused by excessive electrical discharges from a group of brain cells. The characteristics of the seizure vary depending on where in the brain the seizure starts and how far it spreads. As of 2016, approximately 50 million people worldwide currently live with epilepsy and about 70% of people respond positively to the Anti-epileptic drugs (AEDs).

Drug resistant epilepsy is defined by the International League Against Epilepsy (ILAE) as 'failure of adequate trials of two tolerated, appropriately chosen and used antiepileptic drug schedules (whether as monotherapies or in combination) to achieve sustained seizure freedom'[3]. Epilepsy surgery is a safe and effective alternate treatment option. Therefore, epileptic surgery is often considered when two or more drugs do not control the seizures, and the origin of the seizures can be identified and localized to one particular area, epileptogenic zones (EZs)[4], [5], of the brain which can be safely

resected. The concept of EZs was first described by Lüders as ‘the minimum amount of cortex that must be resected (or completely disconnected) surgically to produce seizure freedom’[6][7]. This implies that epileptologists and neurosurgeons that perform the surgery must perform various examinations to determine the EZ. However, oftentimes recorded data maybe too long and too subtle to be identified as a seizure by the human eye. Hence interactions between different areas of the brain can be useful to determines the EZs prior to surgery[6]. Therefore, in this thesis we will discuss the use and accuracy of transfer entropy (TE), a quantity that can measure the interactions between systems while also considering the non-linear and dynamic nature of the systems involved.

Neural disorders are generally studied through Electroencephalography (EEG) signals as they offer an inexpensive and easy way to read the brain activity. Both scalp and intra-cerebral EEG signals[8] are used to convey the activity of the brain during the observation period of the patient [9]. In the context of epilepsy, EEG signals can be used to answer two major questions. Firstly, they determine if the patient has epilepsy. Secondly, they can be used to identify the EZs. Interictal epileptiform discharges (IEDs) in EEG differentiates between an epileptic and non-epileptic brain wave. The presence of these abnormalities are often used to define the epileptic condition, determine the diagnostic and therapeutic approaches as well as provide prognostic information[10]. Rarely does the EEG show false-positive for a normal individual[11].

1.2 EEG Signals:

Electroencephalography (EEG) is a method of monitoring the electrical activity of the brain. It reproduces the cortical activity, which is quite small and measured in microvolts (mV). The recordings are generally noninvasive and collected from the electrodes placed on the scalp. There are also invasive electrodes that are sometimes employed which require surgical placement of the electrodes[12]. EEG electrodes capture the change in voltage caused by the ionic current from the neurons of the brain. They are recorded simultaneously from multiple locations over a period of time.

EEG is important for the diagnosis and treatment of mental and brain neuro-degenerative diseases and abnormalities as well as many neurological disorders. It helps physicians to give an accurate diagnosis. Quantitative EEG is a study of the mathematical processing to the electroencephalogram[13]. Techniques like Independent Component Analysis (ICA) and source localization techniques are used by researchers interested in understanding the source of EEG signals. Neuromodulation, allows the control of EEG signals through audio or visual feedback loops, proved helpful for ADHD and medication aid. Recently, EEG signals are used as a biomarker for neurogenerative diseases. EEG based neuromodulation together with brain stimulation have been proposed for stroke rehabilitation. EEG is popular in brain-computer interface (BCI) applications. EEG signals are also used to study event-related potentials or the spectral content of the EEG. While event-related potentials (ERP) study the small voltages generated in the brain in response to specific events or stimuli[14], spectral analysis is a method used to characterize and analyze the data.

The best-known application of EEG signals is in the detection of epileptic seizures for the localization of the epileptogenic zones (EZs). EEG signal is a combination of different categories of data. Since the data is generally very large, automated methods are necessary to analyze and classify the data. Visual inspection of the EEG signals proves lacking as there are no standard criteria, time-consuming and often results in errors. Thus, provides another challenge in terms of extracting important features for classification.

1.3 Problem Statement:

For drug resistant epilepsies, the location of the origin of the seizure in the brain tells a lot about the kind of treatment that will best suit the seizure type. Based on the onset of the seizures, epileptic seizure zones can be classified into two groups, partial and generalized. As the names suggest, partial seizures affect one particular area of the brain while generalized seizures affect both sides of the brain or a large group of cells at the same time. Thus, it becomes very important for a physician to determine the category of seizures the patient falls under. Locating the area of the brain that is responsible for the seizure makes it easier for surgeons to surgically resect that part of the brain or to place neurostimulators.

The epileptogenic zones consist of five different cortical zones: symptomatogenic, irritative, Ictal onset, epileptogenic lesion and functional deficit zones. A brief summary of the zones along with the respective diagnostic techniques is described in the Table 1-1. It is very easy to identify the epileptogenic zones when all the fine zones point to the same location. However, these five zones are not always present at the same location.

Thus, deciding on the 'true' epileptogenic zone is still a very challenging problem. In this thesis, work has been done on using Transfer Entropy to determine the location of epileptogenic zones in patients. The proposed method is a probabilistic approach to the information transfer between two signals.

Table 1-1. Definitions of the epileptogenic zones and associated diagnostic [13]

Zones	Description	Tests
Epileptogenic	Cortical area generating seizures, removal makes patient seizure-free	Combination of all tests
Symptomatogenic	Cortical area that generates initial seizure symptomatology	Video analysis of seizure semiology
Irritative	Cortical area generating interictal epileptiform discharges	Scalp EEG, invasive recording, ECoG, MEG
Ictal onset (pacemaker)	Cortical area from which seizures can be demonstrated to originate	Video-EEG monitoring (non-invasive/invasive), ictal SPECT
Epileptogenic lesion	Visible structural lesion responsible for generating seizures	High resolution MRI
Functional deficit	Area that shows abnormal function in the interictal state	Neuro exam, Wada test, neuropsychology, interictal PET/SPECT, fMRI, MRS

1.4 Thesis Organization:

Chapter 1 provides an overview of Epilepsy, EEG signals and the problem statement of this thesis which is the use of a non-linear information transfer technique called the transfer entropy to identify Epileptogenic zones. A review of the existing literature on identifying EZs and the advantages provided by using TE are also discussed. Chapter 2 provides the mathematics approach towards the computation of TE and the study of parameters involved in its calculation. Chapter 3 provides the information on the patients that were studied as a part of this thesis. In chapter 4, the data obtained after processing the EEG signals of the patients is explained and the signals of interest are analyzed. A detailed discussion on the effect of changes in parameters and a comparison with correlation matrix is also provided. Chapter 5 summarizes the thesis and provides some discussion on future work.

1.5 Literature Review

Over the past decade, there has been a tremendous increase in the study of neural assemblies [15]–[18] and finding techniques to compute the information transfer[19] and functional connectivity between neurons[20]–[24]. Traditionally these were measured in terms of correlation or mutual information. Correlation measures the similarities between two signals but does not take into account the effect of higher order moments. Mutual information on the other hand accounts for these higher order moments but fails to give any indication of direction of the flow of information due to its symmetry[25]. Therefore, an alternative method called Transfer Entropy was developed which introduces the concept of directed information transfer using a probabilistic approach. It estimates the

activity of the neuron that is independent of its own past activity but dependent on the past activity of another neuron. This method quantifies information flow without any constraints on the underlying model[26], [27] or characteristics of the systems involved. It also incorporates the dynamics of individual system[28]. Thus, making it an effective tool for computing complex neural networks. In the past decade experiments have been conducted where transfer entropy was used in the analysis of EEG signals in both animals and humans. Directed information method also claims to accurately identify the seizure zones[29],[30]. However, for the course of this thesis we will explore Transfer entropy and its accuracy in localizing EZs.

Some work involving depth electrodes has been done to capture artifact free signals for analysis, from the brains of guinea pigs and cats over a small observational window, in addition to looking at EEG signals from the surface of the brain. In the experiment involving auditory cortical neurons in cats[31]–[33], the activity recorded from an array of 16 electrodes in the auditory cortex is analyzed. The results from this experiment show NTE can be used to investigate integration memory as well as information transfer in neural assemblies. Part of this experiment also involves the study of spike train in response to various stimuli which shows that the network remains unchanged with regard to the stimulus used. The experiments involving the epileptic signals in guinea pigs[34], improvements to the TE estimation were made by introducing greedy strategy. This approach however introduces an order-estimated measure to detect connectivity in intercranial EEG signals. TE proved effective in establishing nonlinear information transfer between cortex and basal ganglia for Parkinson's disease[35]. It also plays a

significant role in the identification of biomarkers to identify Mild cognitive impairment (MCI) and Alzheimer's disease (AD) by providing distinguishable features[36]. Research on applying Transfer entropy with self-prediction optimality and graph theory parameters to distinguish between an autistic youth and a healthy youth shows positive results[37].

In this thesis, TE analysis for the data collected from patients with epilepsy is performed. The data is collected by using depth electrodes as we are more interested in locating the focus of the seizure, which generally starts deeper in the brain and spreads outwards. With this presurgical analysis, we aim to identify the seizure zone[38]–[42]. All the patients in this experiment either suffer from a broad generalized location of seizure or from multifocal seizures. Since in these cases epileptic surgery is out of the picture, alternative treatment options like neuro-stimulation devices -responsive neuro-stimulation (RNS) if there are two distinct foci or Vagus nerve stimulation if there are more than two foci or the foci are not well identified can be considered. Thus, making it essential to have a precise idea of the origin of these seizures.

Chapter 2

Transfer Entropy

It is important to measure the extent to which an individual component contributes to information production and the rate at which they exchange information among each other for a multi component system. This given information about the structure of the systems involved. Therefore, a measure that quantifies the statistical coherence between systems becomes essential. Transfer entropy introduces these components in a probabilistic approach and quantifies the directional information transfer between two signals. No constraints are imposed on either the model or the characteristics of the signal, making it an effective tool for nonlinear computations of complex neurological circuits. The mathematical expressions that are used to derive at transfer entropy are discussed in this chapter[43]–[45].

2.1 Discussion of Transfer Entropy:

2.1.1 Transfer Entropy:

Consider a stochastic system where any random variable relies only on the variable preceding it and is conditionally independent of all the other preceding random variables. This system can be approximated as a stationary Markov process of order k, this implies that the conditional probability to find X in state x_{n+1} at time $n+1$ is independent of the state x_{n-k}.

$$p(x_{n+1}|x_n, \dots, x_{n-k+1}) = p(x_{n+1}|x_n, \dots, x_{n-k+1}, x_{n-k}) \qquad \textit{(Eq 2.1)}$$

We will use the notation $x_n^{(k)} = (x_{n+1}|x_n, \dots, x_{n-k+1})$ for words of length k.

When this system is extended to two processes (X, Y) and we measure the deviation from the generalized Markov property that in the absence of information flow from Y to X, the state Y has no influence on the transition probabilities on system X. When the above Markov expression is extended to two independent random processes *x* and *y* we get

$$p\left(x_{t+1}\middle|x_t^k\right) = p(x_{t+1}|x_t^k, y_t^l) \qquad \textit{(Eq 2.2)}$$

The values of the parameters k and l are the orders of the Markov process for the two coupled process X and Y respectively. Where $x_t^k = (x_t, x_{t-1}, x_{t-2}, \dots, x_{t-k+1})^T$ and $y_t^l = (y_t, y_{t-1}, y_{t-2}, \dots, y_{t-l+1})^T$ are the state vectors at time *t*.

The variability of the future state given the past state is given by $log(\frac{1}{p(x_{t+1}|x_t^k)})$. When substituted into the Shannon entropy equation

$$H\left(x_{t+1}\middle|x_t^k\right) = \sum p\left(x_{t+1}, x_t^k\right)\log(\frac{1}{p(x_{t+1}|x_t^k)}) \qquad \textit{(Eq 2.3)}$$

Transfer entropy computes the deviation from the assumption that the dynamics of the process X is explained by its own past and that no influence from the dynamics of process Y is observed on the information gathered from X. It measures the amount of mutual information transfer from *X* to *Y*. This is derived using the Kullback-Leibler divergence:

$$TE_{Y\to X} = H\left(x_{t+1}\middle|x_t^k\right) - H\left(x_{t+1}\middle|x_t^k, y_t^l\right) \qquad \textit{(Eq 2.4)}$$

$$TE_{Y\to X} = \sum_x \sum_y p(x_{t+1}, x_t^k, y_t^l) log \frac{p(x_{t+1}|x_t^k, y_t^l)}{p(x_{t+1}|x_t^k)}$$

$$= \sum_x \sum_y p(x_{t+1}, X_t^k, Y_t^l) log \frac{p(x_{t+1}, x_t^k, y_t^l)p(x_t^k)}{p(x_{t+1}, x_t^k)p(x_{t+1}, x_t^k)}$$

where, $TE_{Y\to X}$ measures the predictability of the future values of X that are given by the past values of X and Y. This can only be done after removing the dependencies between the future and past values of X.

2. 1.2 Normalized Transfer Entropy:

We define the normalized transfer function (NTE) by

$$NTE_{Y\to X} = \frac{TE_{Y\to X} - TE_{Y\to X}^{shuffled}}{H\left(x_{t+1}\middle|x_t^k\right)} \in [0,1] \qquad \textit{(Eq 2.5)}$$

The NTE represents a fraction of information in *X* explained by its own past which is not explained by the past of *Y*. We normalized the data obtained from calibrating TE to reduce data redundancy and to increase the data integrity.

As a part of this thesis, I have computed NTE values at different time shifted values of the two signals to estimate the direction of information flow at different time lags. For example, the value of NTE in the case of two identical signals as well as in the case of two independent signals will always result in zero; indicating no information transfer between the two signals. But the introduction of a delay factor between the two signals could increase the value of NTE for the two identical signals from zero to some small positive value while the value of NTE for two independent signals still remains at zero. For simplicity of most of the calculations in this thesis I assume $k = l = 1$ unless it has been specified. The probability density functions (PDFs) obtained from the data is classified into 10 bins spanning the dynamic range of the signals. I chose 10 bins to allow a good trade-off between PDF resolution and sufficiently large bin count (unless

specified otherwise). To account for artifacts and external disturbances during the collection of electrical signals from the brain the estimated mean of the transfer entropy of the time-shuffled versions is subtracted from each individual value.

2.2 Improving the Computation of Transfer Entropy:

A finite dataset is used to analyze transfer entropy, therefore the selection of values for the parameters such as k and l play an important role in getting reliable values[46]. There is a dependence on the rate of sampling that is used to coarse grain the signals captured from the brain. Changing the bin size also has a significant effect on the output obtained.

2.2.1 Selection of k:

The value of k (order of the driven process) used in the transfer entropy calculation represents the dependence of the current state x_{t+1} on its past k states. Many approaches such as Akaike information criterion (AIC)[47], partial mutual information[48], delayed mutual information, etc. were applied to select a suitable value for the order of the Markov process. Delayed mutual information proves to be a better approach because AIC suffers from overestimation and partial mutual information proves effective for unidirectional flow. Using delayed mutual information, the delay d at which the mutual information of X reaches the maximum for the first time is calculated. This delay corresponds to a period of time when the two states of X are dynamically correlated. This value of d minimizes the KL divergence between the dth and the higher order probabilities of X. This implies that there is minimum information gained about the future of X by using more than d steps in the past. A more practical approach of this method is

to select the order of the driven process based on correlation time constant t_e. It can be defined as the time required for any autocorrelation function (AF) to decrease to $1/e$ of its maximum value (where maximum value of AF is 1).

2.2.2 Selection of l:

The value of l (order of the driving system) was considered to be equal to 1. The reason for this assumption was that the current state of the system produces a significant change in the dynamics of the driven system in a single time step. Larger values of l (l = 2) was also explored in this thesis.

2.2.3 Selection of bin size:

The data obtained from the EEG of the brain is classified into bins that span the dynamic range of the signals. The bin size of the normalized histograms is selected in such a way that it provides a good trade-off between the resolution and large bin counts. In this thesis we found that a bin size of 10 gives a reliable value for transfer entropy. We have also analyzed the effect that increase or decrease in bin size has on value of transfer entropy.

Chapter 3

Experimental Setup

3.1 Patient 1:

This patient suffers from non-lesion temporal lobe epilepsy with bi-temporal independent interictal spikes. He showed symptoms of epilepsy despite surgery. To identify the cause of the seizures, the patient was subjected to Stereo-EEG monitoring. Eight depth electrodes were surgically implanted into the brain and the EEG collected from these electrodes were used for further analysis. The electrodes were symmetrically placed in both hemispheres in the amygdala and hippocampus regions. Visual inspection of the EEG identified seizure activity in the right amygdala and hippocampus. However, on calculating the NTE no visual peaks are observed between any electrodes in the depth of the brain or neocortical surface electrodes on the right hemisphere. In contrast, clear peaks were seen near two points on depth electrodes in the left hemisphere.

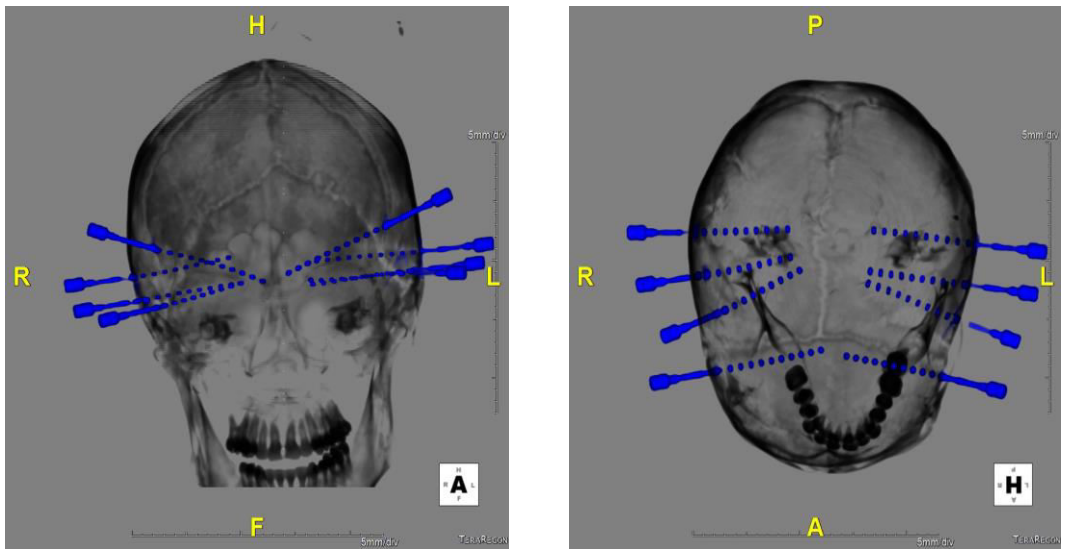

(a) *(b)*

Figure 3-1. Position of depth electrodes in the patient 1 (a) Frontal view, (b) Top view

Figure 3-1. gives the position of the eight electrodes in the brain of the patient. Since they are placed symmetrically there are 40 points on information in both hemispheres. Each of the eight electrodes have ten points of contact. The details about the electrodes and their positions are included in Table 3-1. The position of point 1 of the electrode is at the deepest part of the brain of that particular electrode and point 10 is near the surface of the brain (cortex). This way each signal can be associated with a point of origin in the brain. The spike trains captured from these points can be easily converted into a form that can be processed by the computer.

Table 3-1. Details of electrodes in patient 1

S No	Name of electrode	No of contact	Locations
1.	Left Amygdala (LA)	10	1-10
2.	Left Anterior Hippocampus (LAH)	10	11-20
3.	Left Posterior Hippocampus (LPH)	10	21-30
4.	Left Orbitofrontal (LOF)	10	31-40
5.	Right Amygdala (RA)	10	41-50
6.	Right Anterior Hippocampus (RAH)	10	51-60
7.	Right Posterior Hippocampus (RPH)	10	61-70
8.	Right Orbitofrontal (ROF)	10	71-80

3.2 Patient 2

This patient has constantly experienced seizures since the age of three. He was diagnosed with Mesial temporal sclerosis (MTS) as a result of examining his magnetic resonance. MTS was thought to be the cause of his temporal lobe epilepsy with partial seizure focus. He was initially put on anti-epileptic drugs. Despite changes to his dosage and diet but he still showed symptoms of seizure. Based on the findings from the surface EEG and clinical evaluations, he underwent a standard surgery of the temporal lobe. However, it failed to control his seizures. Before he underwent a second epilepsy surgery he was placed under invasive video-EEG monitoring where multiple electrodes were placed in his brain. All the electrodes were placed on his right hemisphere as the seizures were observed on that side.

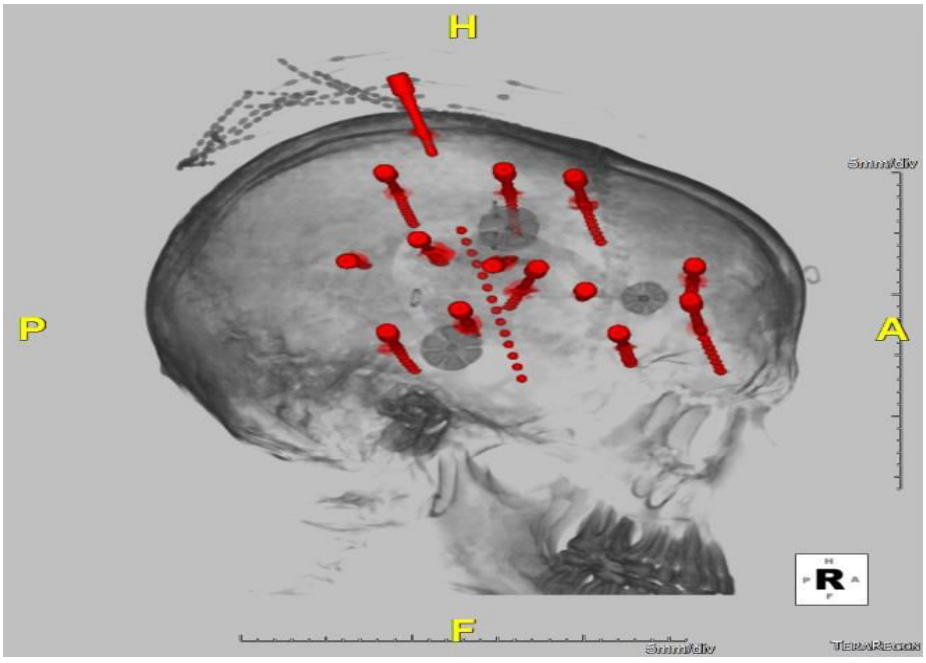

Figure 3-2 Position of depth electrodes in the patient 2

The electrodes, figure 3-2, used in this case have different no of contacts at different depths and locations in the brain. The distance between two points in the electrode is always the same, therefore the length of the electrodes depends on the total distance that the information travels from deeper parts of the brain to the surface. Which implies that if an electrode has higher number of contacts, then the electrode used itself will be longer. The information on the electrodes used for this patient are shown in Table 3-2. The patient was monitored for a total of 19 days.

Table 3-2. Details of electrodes in patient 2

S No	Name of electrode	No of contact	Locations
1.	Angular Gyrus (AG)	4	1-4
2.	Anterior orbitofrontal (AFO)	8	5-12
3.	Face motor (FM)	6	15-20
4.	Frontopolar -cingulate (FPC)	8	21-28
5.	Face sensory (FS)	8	29-36
6.	Hand motor-cingulate (HMC)	10	37-46
7.	Hand sensory-cingulate (HSC)	10	47-56
8.	Insula (INS)	14	55-70
9.	Posterior basal temporal (PBT)	8	71-78
10.	Premotor (PM)	10	79-88

3.3 Patient 3

This patient has experienced seizures from the age of 2. This patient suffers from left arm dystonia and loss of speech caused by seizure episodes. Noninvasive EEG monitoring (Table 3-3) showed seizure activity in the right frontotemporal region. However, PET EEG and MRI showed activity in the left hippocampus region. Due to this ambiguity, invasive EEG was recommended for this patient. The seizure pattern in this patient were classified as complex partial (focal impaired awareness) with secondary generalization (bilateral tonic-clonic seizure).

Table 3-3. Details of electrodes in patient 3

S No	Name of electrode	No of contact	Locations
1.	Left Amygdala (LA)	12	1-12
2.	Left Anterior Hippocampus (LAH)	12	13-24
3.	Left Posterior Hippocampus (LPH)	10	25-34
4.	Left Superior Temporal Gyrus (LSTG)	8	35-42
5.	Left Temporal Pole (LTPOL)	8	43-50
6.	Right Amygdala (RA)	12	51-62
7.	Right Anterior Hippocampus (RAH)	10	63-72
8.	Right Posterior Hippocampus (RPH)	10	73-82
9.	Right Superior Temporal Gyrus (RSTG)	8	83-90
10.	Right Temporal Pole (RTPOL)	10	90-100

3.4 Patient 4

This patient suffers from partial epilepsy arising from the left hemisphere since 2001. His symptoms involve blurry vision, scared feeling and funny feeling. Invasive monitoring shows that the patient's seizures appear on the left temporal (mesial and neocortical) and parietal regions. The information on the electrodes for this patient is shown in Table 3-4.

Table 3-4. Details of electrodes in patient 4

S No	Name of electrode	No of contact	Locations
1.	Left Anterior Hippocampus (LAH)	10	1-10
2.	Left Posterior Hippocampus (LPH)	10	11-20
3.	Anterior Superior Temporal Gyrus (ATI)	6	21-26
4.	Mid Superior Temporal Gyrus (MTI)	6	27-32
5.	Posterior Superior Temporal Gyrus (PTI)	8	33-40
6.	Angular Gyrus (AG)	12	41-52
7.	Supramarginal Gyrus (SMG)	14	53-66
8.	Superior Parietal (SP)	10	67-76
9.	Hand Motor (FM)	12	77-88
10.	Face Motor (FM)	6	89-94
11.	Face Sensory (FS)	14	95-108
12.	Hand Sensory (HS)	14	109-122
13.	Insula (INS)	14	123-136
14.	Isthmus Cingulate Gyrus (ICG)	12	137-148

Chapter 4

Results and Discussion

4.1 Discussion of data grids

The NTE values for each possible pair of signals is computed. The maximum of the NTE values for each pair is selected and a grid of data is generated. This grid shows amount of information transferred during the epileptic seizure. We want to capture electrodes that tend to discharge high erratic electrical signals in the brain. When the intensity of such interactions is plotted, spots that are in deep red or orange shades show highest levels of interaction while dark blue spots represent low levels of interactions. The deep red or orange spots can be interpreted as the point of seizure origin. Finally, the individual signal interactions are plotted to confirm the findings.

4.1.1 Discussion of data grid for patient 1

The data grid that is obtained from patient 1 is shown in figure 4-1 (a). The data is arranged in such a way that the first forty signals on both the axes are collected on the left hemisphere of the brain and the next forty from the right hemisphere. Points 1-10 are contacts of electrode LA, 11-20 of LAH, 21-30 of LPH, 31-40 of LOF, 41-50 of RA, 51-60 of RAH, 61-70 of RPH and 71-80 of ROF. If the grid were to be divided into smaller portions, the top left 40*40 matrix would represent the interaction between the signals in the left hemisphere, similarly the top right shows the interactions of the left hemisphere with right hemisphere, the bottom left shows the interactions between right hemisphere

with left hemisphere and the bottom right shows the interactions between signals in the right hemisphere.

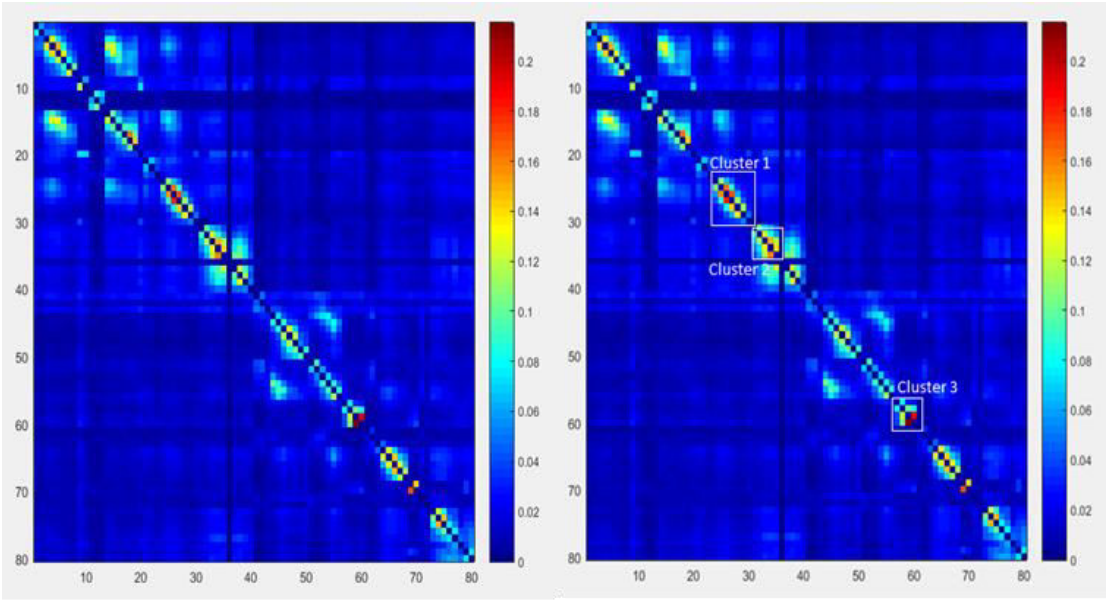

(a) *(b)*

Figure 4-1. (a) Data grid obtained from patient 1, (b) Data grid showing clusters in patient 1

It can be observed that there are no interactions on the top right or the bottom left portion of the grid. This can be interpreted as no interaction between the two hemispheres. Most of the activity is concentrated within the left or right hemisphere. Figure 4-1 (b) shows three clusters of deep red or orange spots can be seen near the diagonal of the matrix. Two of the three are seen on the left hemisphere and one on the right hemisphere. Investigating these spots further, we look into the individual interaction of signals in that cluster. In figure 4-2 (a), (b) we study the interactions in the first cluster which is the interaction of the LPH1 electrode with other electrodes. The peaks present in these signals show higher interactions between the pair of signals considered. Peaks are also observed for the inverse of the same pair of signals. Taking a closer look at cluster 1, the

reason for high interactions on both

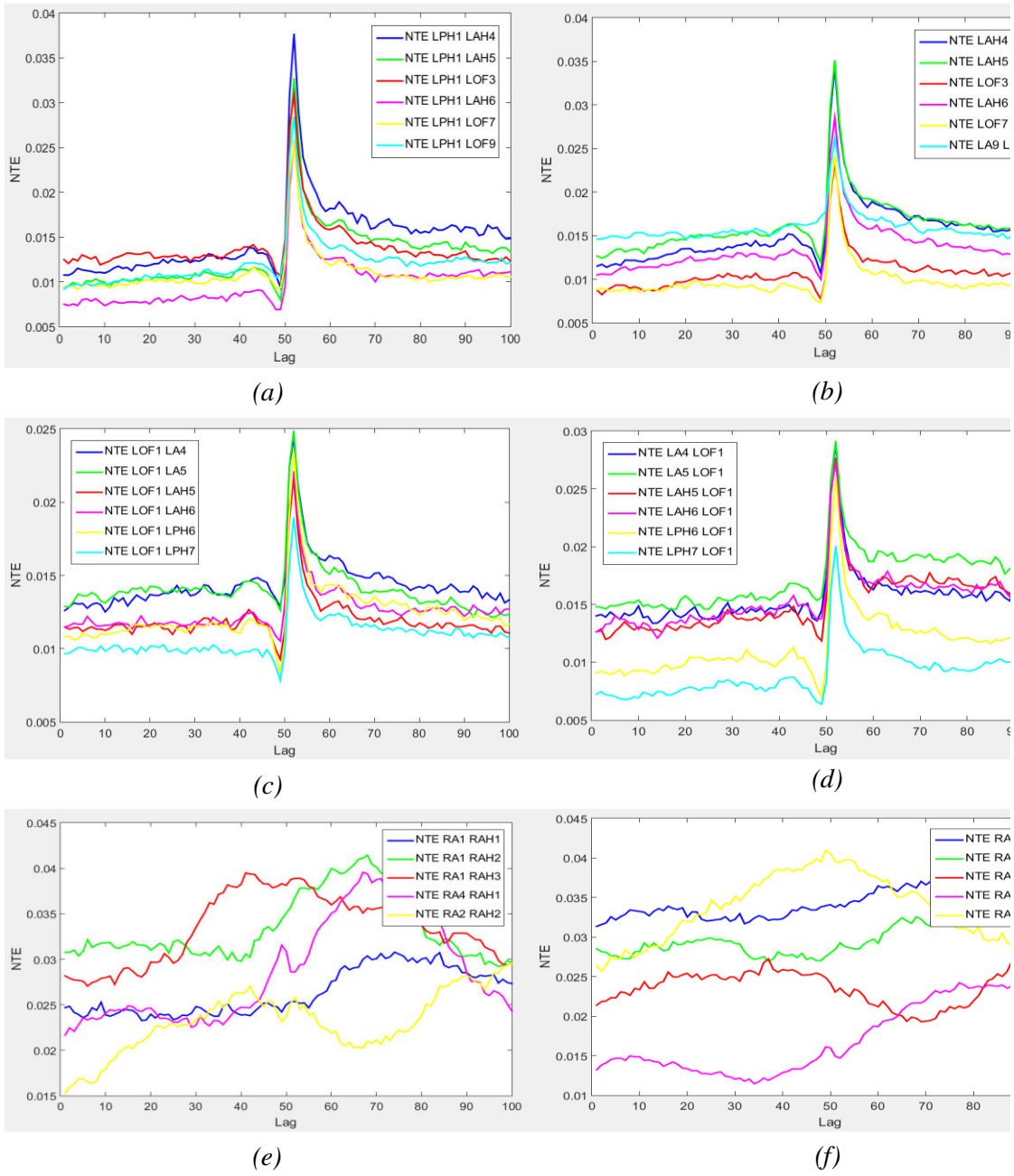

Figure 4-2. (a) Signal showing interactions between LPH1 and other electrodes in cluster 1, (b) Signal showing interactions between other electrodes in cluster 1 and LPH1, (c) Signal showing interactions between LOF1 and other electrodes in cluster 2, (d) Signal showing interactions between other electrodes in cluster 2 and LOF1 (e), (f) Signal showing interactions between electrodes on the right hemisphere in cluster 3

sides can be attributed to symmetry in the cluster. Similarly, the second cluster (figure 4-2 (c), (d)) shows the interaction of the LOF1 electrode with other electrodes. Observing

the third cluster (figure 4-2 (e), (f)) on the right hemisphere however shows no peaks in the NTE calculations. This suggests the presence of noise from artifacts interacting with the signal during capture. Due to the presence of multiple spots on the grid, this patient shows multifocal epilepsy.

The correlation matrix for this patient is shown in figure 4-3. There appears to be no linear interactions between the contacts of the electrodes. No information could be inferred from this matrix, suggests that the information transfer is non-linear.

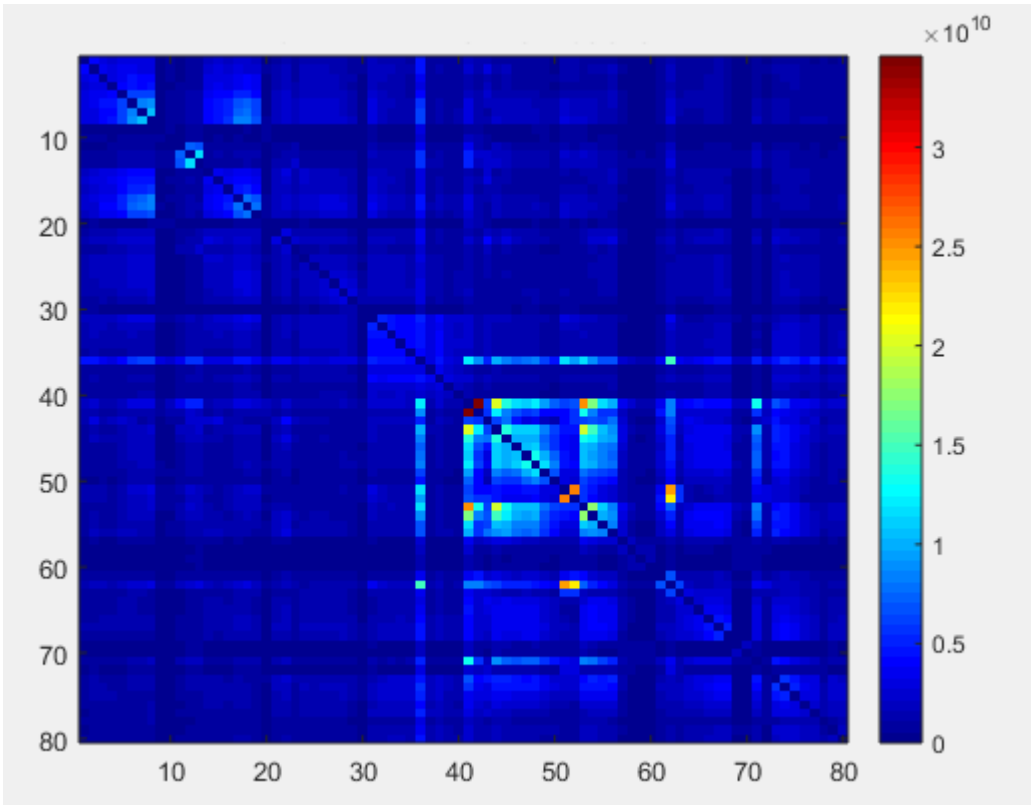

Figure 4-3. Correlation matrix of patient 1

4.1.2 Discussion of data grid for patient 2

The data grid that is obtained from patient 2 is shown in figure 4-4 (a). The data follows the order 1-4 of electrode AG, 5-12 of electrode AFO, 15-20 of electrode FM, 21-28 of electrode FPC, 29-36 of electrode FS, 37-46 of electrode HMC, 47-56 of electrode HSC, 55-70 of electrode INS, 71-78 of electrode PBT, 79-88 of electrode PM, 89-96 of electrode PFO, 97-102 of electrode POI, 102-106 of electrode PT and 107-110 of electrode TI on both the axes.

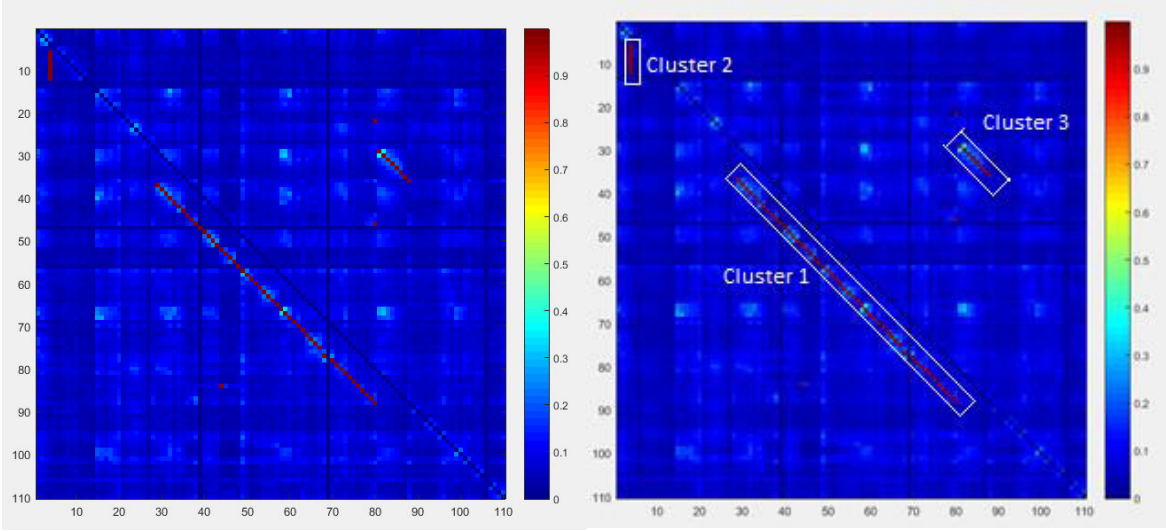

(a) *(b)*

Figure 4-4. (a) Data grid obtained from patient 2, (b) Data grid showing clusters in patient 2

As can be seen from the figure 4-4 (b), three deep red cluster regions are be observed. Taking a closer look at cluster 1, these dark points are the interactions between deep contacts of FS electrode with surface contacts of HCM (Figure 4-5 (b)), deep contacts of HCM with surface contacts of HSC (Figure 4-5 (c)), surface contacts of HCM with deep

contacts of INS (Figure 4-5 (d)). We see that the inverse of these interactions shows no

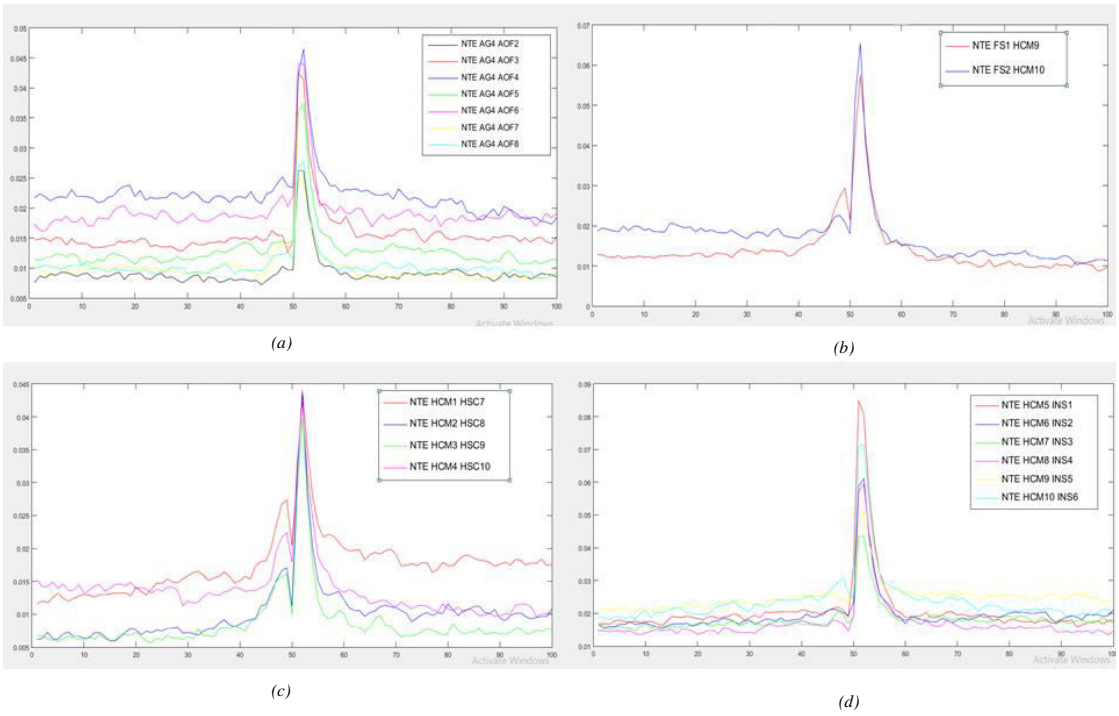

Figure 4-5. (a) Signal showing interactions between AG4 and all points on electrode AOF, (b) Signal showing interactions between deep FS contacts and surface HCM contacts, (c) Signal showing interactions between deep HCM contacts and Surface HSC contacts, (d) Signal showing interactions between deep HCM contacts and Surface INS contacts

peaks. This proves the directionality of the information flow. The dark points in cluster 2 is the interactions between all the points of contact on the AOF electrode with one of the surface contact of the AG electrode (AG4) (Figure 4-5 (a)). Here, we are more focused on analyzing cluster 1 as it points to a large area of the brain. Since there is generalized area of the brain that is responsible for the seizure, this patient has no isolated EZ that could be resected. Correlation matrix is shown in figure 4-6.

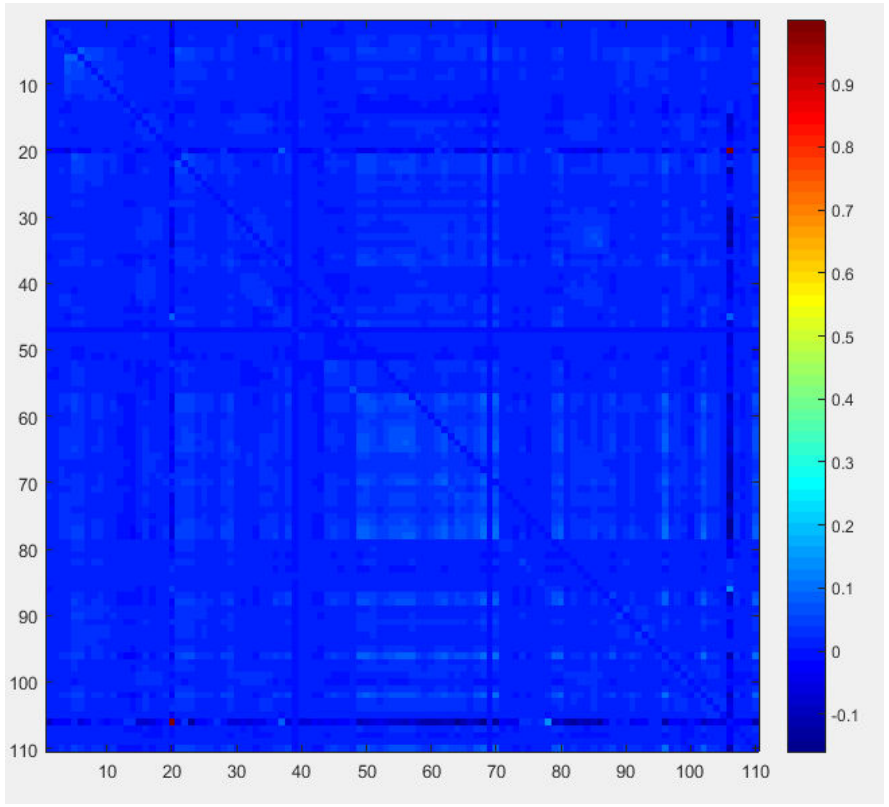

Figure 4-6. Correlation matrix of patient 2

4.1.3 Discussion of data grid for patient 3

The data grid that is obtained from patient 3 is shown in figure 4-7 (a). The data is arranged in such a way that the first fifty signals on both the axes are collected on the left hemisphere of the brain and the next fifty from the right hemisphere. Points 1-12 are contacts of electrode LA, 13-24 of LAH, 25-34 of LPH, 35-42 of LSTG,43-50 of LTPOL, 41-50 of RA, 51-60 of RAH, 61-70 of RPH and 71-80 of ROF. If the grid were to be divided into smaller portions, the top left 50*50 matrix would represent the interaction between the signals in the left hemisphere, similarly the top right shows the interactions of the left hemisphere with right hemisphere, the bottom left shows the

interactions between right hemisphere with left hemisphere and the bottom right shows the interactions between signals in the right hemisphere.

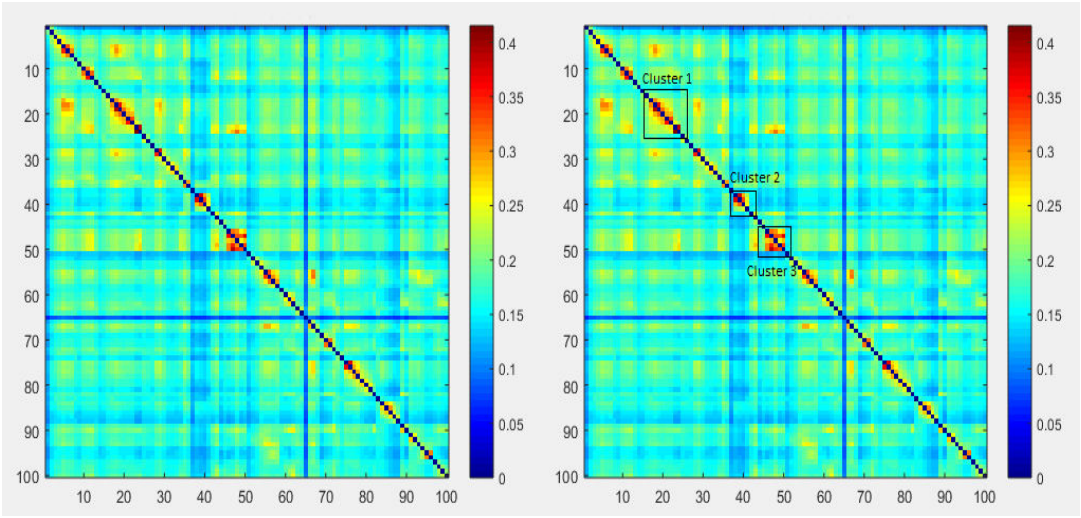

Figure 4-7. (a) Data grid obtained from patient 3, (b) Data grid showing clusters in patient 3

It can be observed that there are no interactions on the top right or the bottom left portion of the grid. This can be interpreted as no interaction between the two hemispheres. Most of the activity is concentrated within the left hemisphere. Figure 4-7 (b) shows three clusters of deep red or orange spots can be seen near the diagonal of the matrix. All of them are observed on the left hemisphere. Taking a closer look (figure 4-8 (a), (b), (c)), all three clusters are formed by interactions between the depth electrodes of LAH (6-11), LSTG (4-6) and LTPOL (4-8) respectively. The presence of three spots which show positive seizure activity lead to a conclusion that this patient has multifocal epilepsy. The Correlation matrix for this patient is shown in figure 4-8 (d).

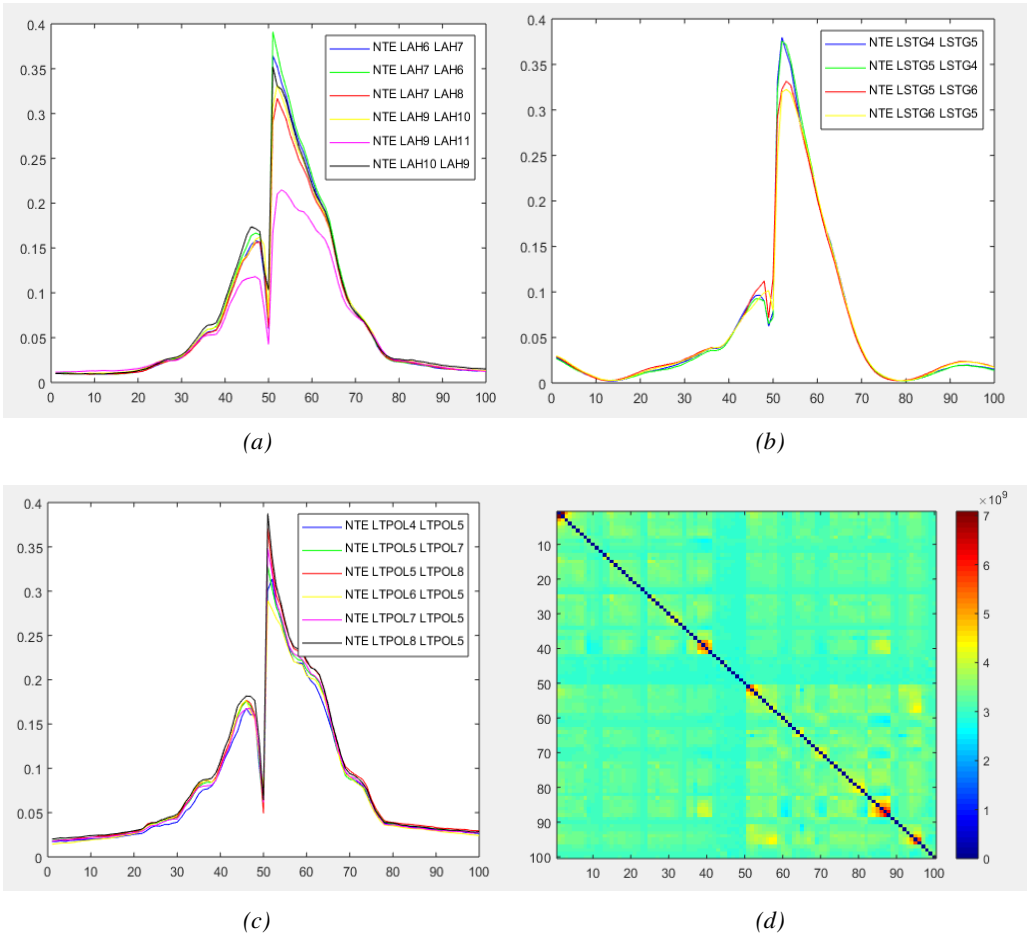

Figure 4-8. (a) Signal showing interactions between LAH 6-11,
(b) Signal showing interactions between LSTG 4-6,
(c) Signal showing interactions between LTPOL 4-8,
(d) Correlation matrix for patient 3

4.1.4 Discussion of data grid for patient 4

The data grid that is obtained from patient 4 is shown in figure 4-9. The data is collected from the left hemisphere of the brain. The points are arranged as 1-10 are from electrode LAH, 11-20 from electrode LPH, 21-26 from electrode ATI, 27-32 from electrode MTI, 33-40 from electrode PTI, 41-52 from electrode AG, 53-66 from electrode SMG, 67-76 from electrode SP, 77-88 from electrode FM, 89-94 from electrode FM, 95-108 from

electrode FS, 109-122 from electrode HS, 123-136 from electrode INS and 136-158 from electrode ICG.

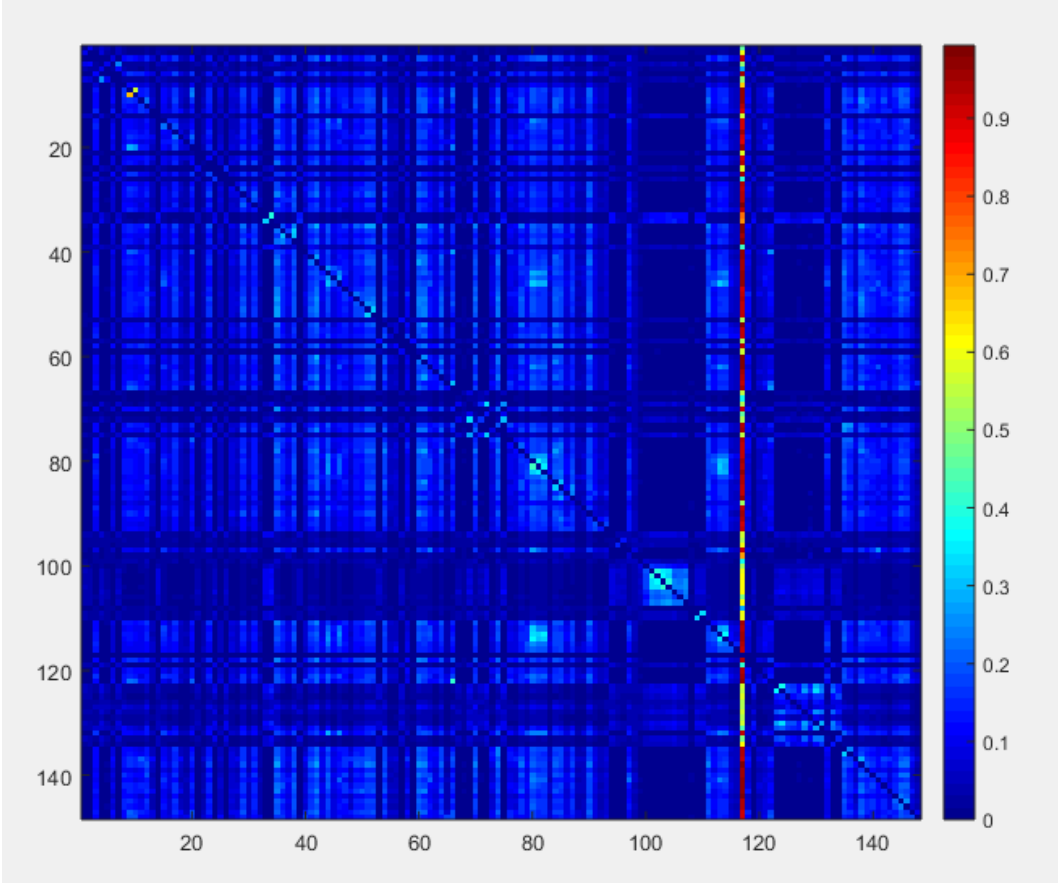

Figure 4-9. Data grid obtained from patient 4

From the figure 4-9 it can be observed that only one electrode interacts (HS9) with all other electrodes (Figure 4-10 (a), (b)). Figure 4-10 (c) shows interactions between HS9 and FS contacts, since the figure doesn't show high interactions (yellow spots instead of red spots) there are no peaks observed here. Due to evidence of seizure on multiple electrode, this patient is not considered for resective surgery, however he may benefit from responsive neurostimulation. The aim in this case is to identify the region responsible for the seizures.

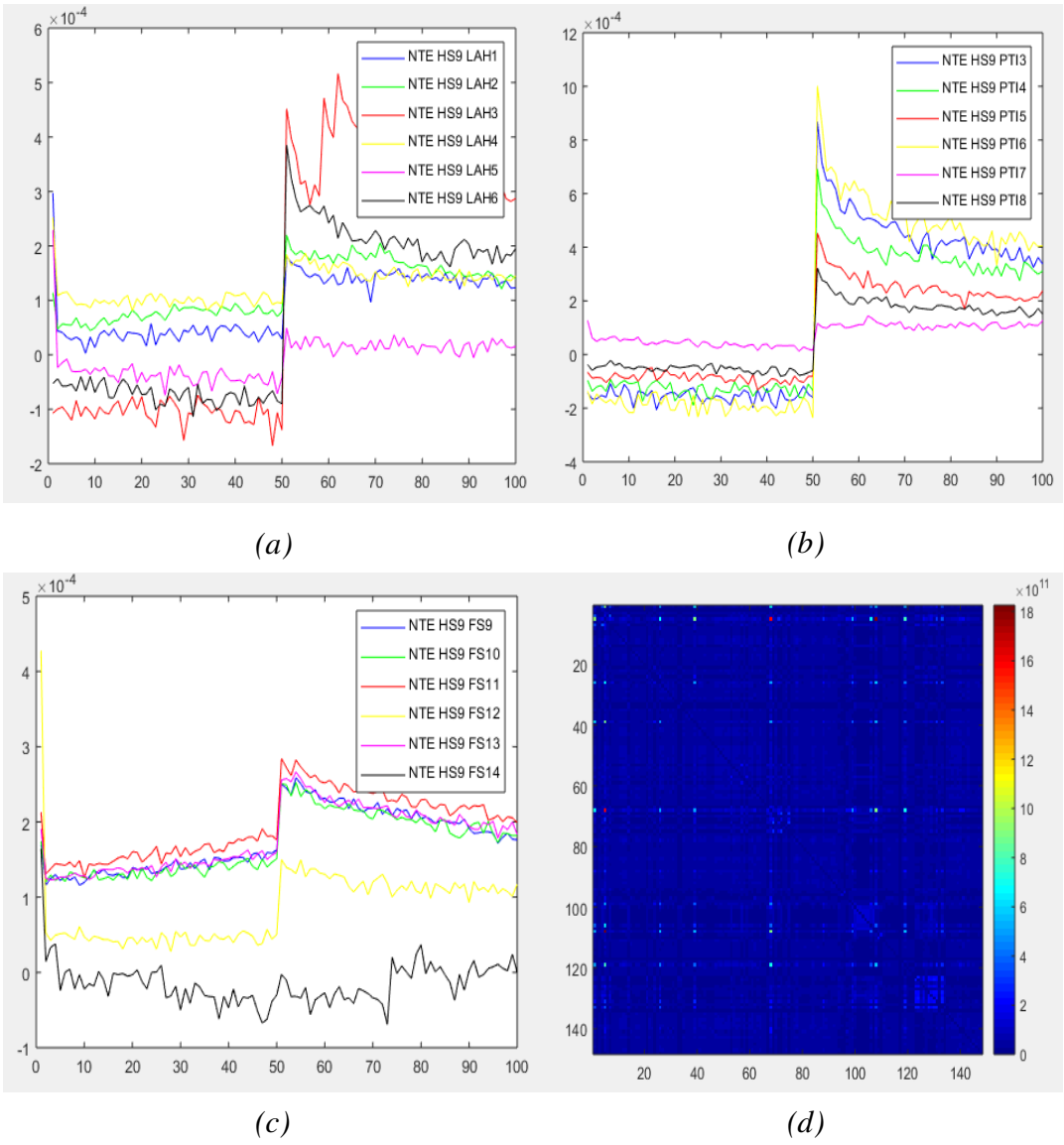

Figure 4-10. (a) Signal showing interactions between HS9 and LAH contacts,
(b) Signal showing interactions between HS9 and PTI contacts,
(c) Signal showing interactions between HS9 and FS contacts,
(d) Correlation matrix for patient 4

4.2 Changing bin sizes

The ideal bin size of 10 was considered thus far in evaluating the NTE data. Exploring the effect of change in bin size is a part of this thesis. The experiment was conducted on patient 1 for varying values of bin size (8,20,25). The corresponding data grids are shown in figure 4-11. As seen, there is not much difference in the data that is obtained in each case. Thus, concluding that there is not much effect of bin size on the data.

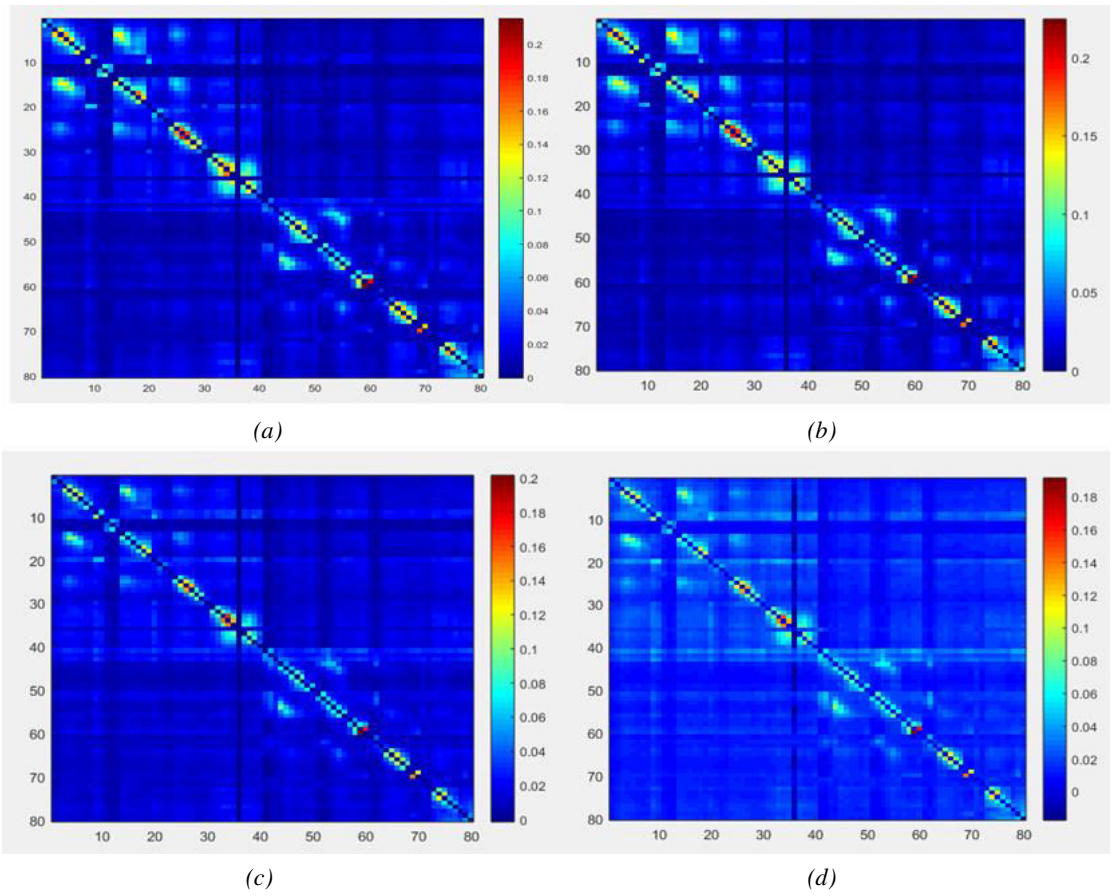

Figure 4-11. Data grid for different bin sizes (a) bin size = 10, (b) bin size = 8, (c) bin size =20, (d) bin size = 25

4.3 Changing *k, l* parameters

We have considered two cases while changing the parameters. Case 1, k=2 and l=1 (figure 4-12 (a)). For this case the NTE of the future value of x depends on previous two states of x and one previous state of y. The grid is shown in figure. Every contact shows high interactions. Inferring from the figure, NTE is sensitive to the change in the parameter k. Case 2, l=2 and k=1 (figure 4-12 (b)). For this case the NTE of the future value of x depends on previous two states of y and one previous state of x. The grid is shown in figure. There is no major difference that is observed in the calculation of NTE. Thus, our initial assumption k=1 and l=1 is a good assumption for calculation of NTE.

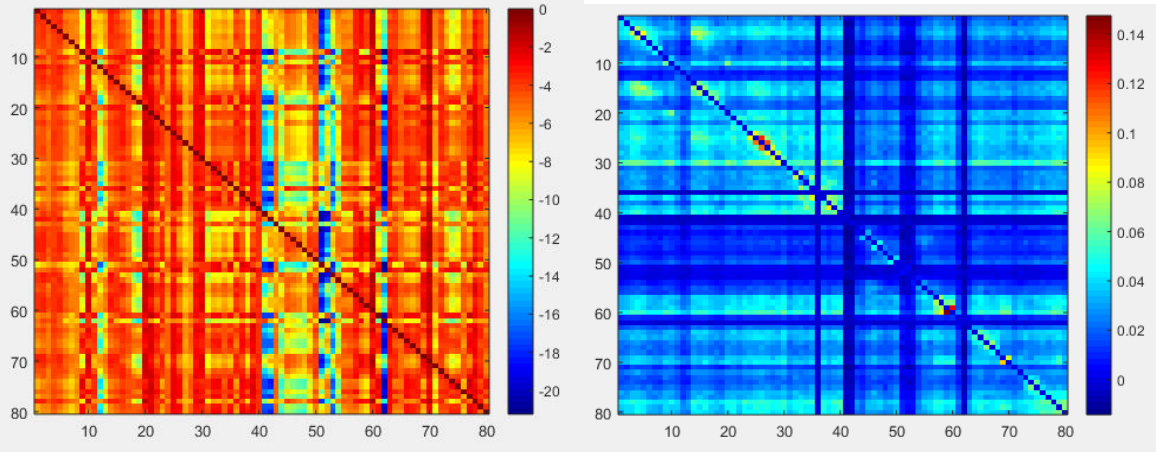

(a) *(b)*

Figure 4-12. Data grid for different Markov order(a) k=2, l=1, (b) k=1, l=2

Chapter 5

Summary and Future work

5.1 Summary

In this research, we study the use of non-linear information transfer technique called Transfer Entropy on Epileptic EEG signals. We used deep intra-cerebral to collect the electrical activity of the brain. These electrodes provide a much clear picture of the activity of the brain when compared to surface EEG monitoring. With this data we intended to locate the Epileptogenic zones that are responsible for the seizure. We apply the NTE algorithm to the data obtained, when the computed results are pulled together in a grid, we look for points on that grid that interact highly with the other points and identify them as epileptogenic zones. With this information we hope to reduce the cost of expensive treatment or surgeries that can be avoided.

As a part of this thesis, we study this method on four different patients of epilepsy. The data for two of the patients showed multiple spots that were highly active during the seizure, thus leading to the conclusion that patient 1 and patient 3 suffer from multi-focal epilepsy. The other two patients had a large cluster of points that were responsible for the seizure. These cases can be classified as generalized epilepsy. These clusters are too large to be considered for surgery, hence alternative treatment in terms of Vagus nerve stimulation can be offered. We also analyzed the effect of changing the parameters such as the bin size and the order of the Markov processes involved. The result of this analysis

proves that our initial assumption on the calculation of NTE has no bias and this model will hold true for all conditions.

5.2 Future Work

With the increase in research interest in neural networks, NTE or any other non-linear information transfer matric will provide a better understanding on the functional connectivity of the brain. This method can be extended to understand similar neurological disorders like Parkinson's[35], Autism[37], disorder of consciousness[49], etc. There can be considerable amount of work done in identifying the electrodes that have captured the seizure using Short-term Fourier Transform (STFT)[50], wavelet[51] or sparse analysis on the EEG data. This will considerably reduce the amount of time that is taken to compute the NTE values for the contacts that do not show any kind of seizure activity. Lastly, to visualize the seizure a 3D model can be constructed of the seizure over the observation time to see the pattern in which seizure spreads in the brain of a patient

References

[1] U. C. Ogbu and O. A. Arah, "World Health Organization," *International Encyclopedia of Public Health*, 2016. [Online]. Available: https://www.who.int/news-room/fact-sheets/detail/epilepsy.

[2] P. Van Mierlo *et al.*, "Functional brain connectivity from EEG in epilepsy: Seizure prediction and epileptogenic focus localization," *Prog. Neurobiol.*, vol. 121, pp. 19–35, 2014.

[3] K. R. Muñana, "Management of Refractory Epilepsy," *Top. Companion Anim. Med.*, vol. 28, no. 2, pp. 67–71, 2013.

[4] L. D. Iasemidis, "Epileptic seizure prediction and control," *IEEE Trans. Biomed. Eng.*, vol. 50, no. 5, pp. 549–558, 2003.

[5] K. Tsakalis and L. Iasemidis, "Control aspects of a theoretical model for epileptic seizures," *Int. J. Bifurc. Chaos*, vol. 16, no. 07, pp. 2013–2027, 2006.

[6] F. Rosenow and H. Lüders, "Presurgical evaluation of epilepsy," *Brain*, vol. 124, no. 9, pp. 1683–1700, 2001.

[7] N. Hitiris, R. Mohanraj, J. Norrie, G. J. Sills, and M. J. Brodie, "Predictors of pharmacoresistant epilepsy," *Epilepsy Res.*, vol. 75, no. 2–3, pp. 192–196, 2007.

[8] M. Wang *et al.*, "Identification of the epileptogenic zone of temporal lobe epilepsy from stereo-electroencephalography signals: A phase transfer entropy and graph theory approach," *NeuroImage Clin.*, vol. 16, pp. 184–195, 2017.

[9] A. Nicoll and C. Blakemore, "Patterns of local connectivity in the neocortex," *Neural Comput.*, vol. 5, no. 5, pp. 665–680, 1993.

[10] J. Engel, "A Practical Guide for Routine EEG Studies in Epilepsy," *J. Clin.*

Neurophysiol., vol. 1, no. 2, 1984.

[11] S. Noachtar and J. Rémi, "The role of EEG in epilepsy: A critical review," *Epilepsy Behav.*, vol. 15, no. 1, pp. 22–33, 2009.

[12] F. Wendling, A. Hernandez, J.-J. Bellanger, P. Chauvel, and F. Bartolomei, "Interictal to ictal transition in human temporal lobe epilepsy: insights from a computational model of intracerebral EEG," *J. Clin. Neurophysiol.*, vol. 22, no. 5, p. 343, 2005.

[13] J. D. Kropotov, *Quantitative EEG, event-related potentials and neurotherapy*. Academic Press, 2010.

[14] S. Sur and V. K. Sinha, "Event-related potential: An overview.," *Ind. Psychiatry J.*, vol. 18, no. 1, pp. 70–73, 2009.

[15] S. P. Strong, R. Koberle, R. R. de R. van Steveninck, and W. Bialek, "Entropy and information in neural spike trains," *Phys. Rev. Lett.*, vol. 80, no. 1, p. 197, 1998.

[16] A. Borst and F. E. Theunissen, "Information theory and neural coding," *Nat. Neurosci.*, vol. 2, no. 11, p. 947, 1999.

[17] G. L. Gerstein and K. L. Kirkland, "Neural assemblies: technical issues, analysis, and modeling," *Neural Networks*, vol. 14, no. 6–7, pp. 589–598, 2001.

[18] B. Gourévitch, R. Le Bouquin-Jeannès, and G. Faucon, "Linear and nonlinear causality between signals: methods, examples and neurophysiological applications," *Biol. Cybern.*, vol. 95, no. 4, pp. 349–369, 2006.

[19] C. Yang, R. L. B. Jeannès, G. Faucon, and H. Shu, "Extracting information on flow direction in multivariate time series," *IEEE Signal Process. Lett.*, vol. 18, no. 4, pp. 251–254, 2011.

[20] A. Pouget, P. Dayan, and R. Zemel, “Information processing with population codes,” *Nat. Rev. Neurosci.*, vol. 1, no. 2, p. 125, 2000.

[21] D. H. Perkel and T. H. Bullock, “Neural coding.,” *Neurosci. Res. Program Bull.*, 1968.

[22] R. C. Decharms and A. Zador, “Neural representation and the cortical code,” *Annu. Rev. Neurosci.*, vol. 23, no. 1, pp. 613–647, 2000.

[23] J. J. Eggermont, “Is there a neural code?,” *Neurosci. Biobehav. Rev.*, vol. 22, no. 2, pp. 355–370, 1998.

[24] B. Hellwig, “A quantitative analysis of the local connectivity between pyramidal neurons in layers 2/3 of the rat visual cortex,” *Biol. Cybern.*, vol. 82, no. 2, pp. 111–121, 2000.

[25] R. Moddemeijer, “On estimation of entropy and mutual information of continuous distributions,” *Signal Processing*, vol. 16, no. 3, pp. 233–248, 1989.

[26] R. Vicente, M. Wibral, M. Lindner, and G. Pipa, “Transfer entropy—a model-free measure of effective connectivity for the neurosciences,” *J. Comput. Neurosci.*, vol. 30, no. 1, pp. 45–67, 2011.

[27] P. Stoica and Y. Selen, “Model-order selection: a review of information criterion rules,” *IEEE Signal Process. Mag.*, vol. 21, no. 4, pp. 36–47, 2004.

[28] J. A. Feldman, “Dynamic connections in neural networks,” *Biol. Cybern.*, vol. 46, no. 1, pp. 27–39, 1982.

[29] R. Malladi, G. Kalamangalam, N. Tandon, and B. Aazhang, “Identifying seizure onset zone from the causal connectivity inferred using directed information,” *IEEE J. Sel. Top. Signal Process.*, vol. 10, no. 7, pp. 1267–1283, 2016.

[30] C. Wilke, W. Van Drongelen, M. Kohrman, and B. He, "Neocortical seizure foci localization by means of a directed transfer function method," *Epilepsia*, vol. 51, no. 4, pp. 564–572, 2010.

[31] D. D. Gehr, H. Komiya, and J. J. Eggermont, "Neuronal responses in cat primary auditory cortex to natural and altered species-specific calls," *Hear. Res.*, vol. 150, no. 1–2, pp. 27–42, 2000.

[32] B. Gourévitch and J. J. Eggermont, "Evaluating information transfer between auditory cortical neurons," *J. Neurophysiol.*, 2007.

[33] B. Gourévitch and J. J. Eggermont, "The spatial representation of neural responses to natural and altered conspecific vocalizations in cat auditory cortex," *J. Neurophysiol.*, 2007.

[34] C. Yang, R. L. B. Jeannès, J.-J. Bellanger, and H. Shu, "A new strategy for model order identification and its application to transfer entropy for EEG signals analysis," *IEEE Trans. Biomed. Eng.*, vol. 60, no. 5, pp. 1318–1327, 2013.

[35] T. P. Gilmour *et al.*, "Transfer entropy between cortical and basal ganglia electrophysiology," in *2012 IEEE Signal Processing in Medicine and Biology Symposium (SPMB)*, 2012, pp. 1–5.

[36] J. McBride, X. Zhao, N. Munro, G. Jicha, C. Smith, and Y. Jiang, "Discrimination of mild cognitive impairment and Alzheimer's disease using transfer entropy measures of scalp EEG," *J. Healthc. Eng.*, vol. 6, no. 1, pp. 55–70, 2015.

[37] A. Dejman, A. Khadem, and A. Khorrami, "Exploring the disorders of brain effective connectivity network in ASD: A case study using EEG, transfer entropy, and graph theory," in *2017 Iranian Conference on Electrical Engineering (ICEE)*,

2017, pp. 8–13.

[38] S. Sabesan, K. Narayanan, A. Prasad, L. D. Iasemidis, A. Spanias, and K. Tsakalis, “Information flow in coupled nonlinear systems: Application to the epileptic human brain,” in *Data Mining in Biomedicine*, Springer, 2007, pp. 483–503.

[39] S. Sabesan, L. B. Good, K. S. Tsakalis, A. Spanias, D. M. Treiman, and L. D. Iasemidis, “Information flow and application to epileptogenic focus localization from intracranial EEG,” *IEEE Trans. neural Syst. Rehabil. Eng.*, vol. 17, no. 3, pp. 244–253, 2009.

[40] K. Lin, Y. Wang, K. Xu, J. Zhu, J. Zhang, and X. Zheng, “Localizing seizure onset zone by convolutional transfer entropy from iEEG,” in *2016 38th Annual International Conference of the IEEE Engineering in Medicine and Biology Society (EMBC)*, 2016, pp. 6335–6338.

[41] P. Kale, J. V. Acharya, J. Acharya, T. Subramanian, and M. Almekkawy, “Normalized Transfer Entropy as a Tool to Identify Multisource Functional Epileptic Networks,” in *2018 40th Annual International Conference of the IEEE Engineering in Medicine and Biology Society (EMBC)*, 2018, pp. 1218–1221.

[42] P. Kale, T. Gilmour, V. J. Acharya, J. Acharya, T. Subramanian, and M. Almekkawy, “Prediction of multifocal epileptogenic zones using normalized transfer entropy,” in *2017 IEEE Signal Processing in Medicine and Biology Symposium (SPMB)*, 2017, pp. 1–4.

[43] T. M. Cover and J. A. Thomas, *Elements of information theory*. John Wiley & Sons, 2012.

[44] T. Schreiber, “Measuring Information Transfer,” *Phys. Rev. Lett.*, vol. 85, no. 2,

pp. 461–464, Jul. 2000.

[45] R. M. Gray, *Entropy and information theory*. Springer Science & Business Media, 2011.

[46] R. W. Katz, "On some criteria for estimating the order of a Markov chain," *Technometrics*, vol. 23, no. 3, pp. 243–249, 1981.

[47] H. Akaike, "A new look at the statistical model identification," in *Selected Papers of Hirotugu Akaike*, Springer, 1974, pp. 215–222.

[48] J. Zhu, R. L. B. Jeannès, C. Yang, J.-J. Bellanger, and H. Shu, "Partial mutual information for simple model order determination in multivariate EEG signals and its application to transfer entropy," in *2012 IEEE International Conference on Acoustics, Speech and Signal Processing (ICASSP)*, 2012, pp. 673–676.

[49] V. Mäki-Marttunen, J. M. Cortes, M. F. Villarreal, and D. R. Chialvo, "Disruption of transfer entropy and inter-hemispheric brain functional connectivity in patients with disorder of consciousness," *BMC Neurosci.*, vol. 14, no. 1, p. P83, Jul. 2013.

[50] K. Samiee, P. Kovacs, and M. Gabbouj, "Epileptic seizure classification of EEG time-series using rational discrete short-time Fourier transform," *IEEE Trans. Biomed. Eng.*, vol. 62, no. 2, pp. 541–552, 2015.

[51] H. Adeli, Z. Zhou, and N. Dadmehr, "Analysis of EEG records in an epileptic patient using wavelet transform," *J. Neurosci. Methods*, vol. 123, no. 1, pp. 69–87, 2003.